

Manipulating the plasmon-induced transparency in terahertz metamaterials

Zhongyang Li,¹ Yingfang Ma,¹ Ran Huang,² Ranjan Singh,^{2,3} Jianqiang Gu,¹ Zhen Tian,¹ Jianguang Han,^{1,4} and Weili Zhang^{1,2,5}

¹Center for Terahertz Waves and College of Precision Instrument and Optoelectronics Engineering, Key Laboratory of Opto-Electronics Information and Technical Science, Ministry of Education, Tianjin University, China

²School of Electrical and Computer Engineering, Oklahoma State University, Stillwater, Oklahoma 74078, USA

³Center for Integrated Nanotechnologies, Materials Physics and Applications Division, Los Alamos National Laboratory, Los Alamos, New Mexico 87545, USA

⁴jiaghan@tju.edu.cn

⁵weili.zhang@okstate.edu

Abstract: Coupling between superradiant and subradiant mode resonators in a metamaterial unit cell plays an important role in observing the sharp transparency peak due to destructive interference between the resonators. This effect is enhanced as the resonators are brought closer to each other in a conventional planar arrangement. We present a novel coupling scheme of planar terahertz metamaterial to tune the plasmon-induced transparency peak by physically varying the distance between the superradiant and the subradiant resonators in such a way that the transparency peak begins to disappear as the coupled resonators are brought closer than a critical separation distance. The effect is attributed to the disappearance of the resonant behavior of the subradiant resonator in a closely coupled regime. The simple planar design presented here demonstrates a scheme to manipulate the electromagnetically induced transparency-like behavior in terahertz metamaterials and this could lead to the development of unique slow light devices for terahertz applications.

© 2011 Optical Society of America

OCIS codes: (160.3918) Metamaterials; (240.6680) Surface plasmons.

References and links

1. S. E. Harris, "Electromagnetically induced transparency," *Phys. Today* **50**(7), 36–42 (1997).
2. T. F. Krauss, "Why do we need slow light," *Nat. Photonics* **2**(8), 448–450 (2008).
3. M. Fleischhauer, A. Imamoglu, and J. P. Marangos, "Electromagnetically induced transparency: optics in coherent media," *Rev. Mod. Phys.* **77**(2), 633–673 (2005).
4. N. Papisimakis, V. A. Fedotov, N. I. Zheludev, and S. L. Prosvirnin, "Metamaterial analog of electromagnetically induced transparency," *Phys. Rev. Lett.* **101**(25), 253903 (2008).
5. S. Zhang, D. A. Genov, Y. Wang, M. Liu, and X. Zhang, "Plasmon-induced transparency in metamaterials," *Phys. Rev. Lett.* **101**(4), 047401 (2008).
6. R. Singh, C. Rockstuhl, F. Lederer, and W. Zhang, "Coupling between a dark and a bright eigenmode in a terahertz metamaterial," *Phys. Rev. B* **79**(8), 085111 (2009).
7. P. Tassin, L. Zhang, T. Koschny, E. N. Economou, and C. M. Soukoulis, "Low-loss metamaterials based on classical electromagnetically induced transparency," *Phys. Rev. Lett.* **102**(5), 053901 (2009).
8. S.-Y. Chiam, R. Singh, C. Rockstuhl, F. Lederer, W. Zhang, and A. Bettiol, "Analogue of electromagnetically induced transparency in a terahertz metamaterial," *Phys. Rev. B* **80**(15), 153103 (2009).
9. N. Liu, L. Langguth, T. Weiss, J. Kästel, M. Fleischhauer, T. Pfau, and H. Giessen, "Plasmonic analogue of electromagnetically induced transparency at the Drude damping limit," *Nat. Mater.* **8**(9), 758–762 (2009).
10. C.-Y. Chen, I.-W. Un, N.-H. Tai, and T.-J. Yen, "Asymmetric coupling between subradiant and superradiant plasmonic resonances and its enhanced sensing performance," *Opt. Express* **17**(17), 15372–15380 (2009).
11. A. Christ, O. J. F. Martin, Y. Ekinci, N. A. Gippius, and S. G. Tikhodeev, "Symmetry breaking in a plasmonic metamaterial at optical wavelength," *Nano Lett.* **8**(8), 2171–2175 (2008).
12. V. A. Fedotov, M. Rose, S. L. Prosvirnin, N. Papisimakis, and N. I. Zheludev, "Sharp trapped-mode resonances in planar metamaterials with a broken structural symmetry," *Phys. Rev. Lett.* **99**(14), 147401 (2007).
13. C. L. Garrido Alzar, M. A. G. Martinez, and P. Nussenzveig, "Classical analog of electromagnetically induced transparency," *Am. J. Phys.* **70**(1), 37–41 (2002).

14. R. Singh, I. A. I. Al-Naib, M. Koch, and W. Zhang, "Sharp Fano resonances in THz metamaterials," *Opt. Express* **19**(7), 6312–6319 (2011).
15. J. Zhang, S. Xiao, C. Jeppesen, A. Kristensen, and N. A. Mortensen, "Electromagnetically induced transparency in metamaterials at near-infrared frequency," *Opt. Express* **18**(16), 17187–17192 (2010).
16. H. A. Haus, *Waves and Fields in Optoelectronics* (Prentice Hall, 1983).
17. Q. Bai, C. Liu, J. Chen, C. Cheng, M. Kang, and H.-T. Wang, "Tunable slow light in semiconductor metamaterial in a broad terahertz regime," *J. Appl. Phys.* **107**(9), 093104 (2010).
18. V. Yannopoulos, E. Paspalakis, and N. V. Vitanov, "Electromagnetically induced transparency and slow light in an array of metallic nanoparticles," *Phys. Rev. B* **80**(3), 035104 (2009).
19. N. Papisimakis, Y. H. Fu, V. A. Fedotov, S. L. Prosvirnin, D. P. Tsai, and N. I. Zheludev, "Metamaterial with polarization and direction insensitive resonant transmission response mimicking electromagnetically induced transparency," *Appl. Phys. Lett.* **94**(21), 211902 (2009).
20. Y. Lu, X. Jin, H. Zheng, Y. P. Lee, J. Y. Rhee, and W. H. Jang, "Plasmonic electromagnetically-induced transparency in symmetric structures," *Opt. Express* **18**(13), 13396–13401 (2010).
21. Y. Lu, J. Y. Rhee, W. H. Jang, and Y. P. Lee, "Active manipulation of plasmonic electromagnetically-induced transparency based on magnetic plasmon resonance," *Opt. Express* **18**(20), 20912–20917 (2010).
22. R. D. Kekatpure, E. S. Barnard, W. Cai, and M. L. Brongersma, "Phase-coupled plasmon-induced transparency," *Phys. Rev. Lett.* **104**(24), 243902 (2010).
23. B. Luk'yanchuk, N. I. Zheludev, S. A. Maier, N. J. Halas, P. Nordlander, H. Giessen, and C. T. Chong, "The Fano resonance in plasmonic nanostructures and metamaterials," *Nat. Mater.* **9**(9), 707–715 (2010).
24. R. Singh, A. K. Azad, J. F. O'Hara, A. J. Taylor, and W. Zhang, "Effect of metal permittivity on resonant properties of terahertz metamaterials," *Opt. Lett.* **33**(13), 1506–1508 (2008).
25. A. K. Azad, J. Dai, and W. Zhang, "Transmission properties of terahertz pulses through subwavelength double split-ring resonators," *Opt. Lett.* **31**(5), 634–636 (2006).
26. R. Singh, C. Rockstuhl, F. Lederer, and W. Zhang, "The impact of nearest neighbor interaction on the resonances in terahertz metamaterials," *Appl. Phys. Lett.* **94**(2), 021116 (2009).
27. P. Tassin, L. Zhang, T. Koschny, E. N. Economou, and C. M. Soukoulis, "Planar designs for electromagnetically induced transparency in metamaterials," *Opt. Express* **17**(7), 5595–5605 (2009).
28. K. L. Tsakmakidis, M. S. Wartak, J. J. H. Cook, J. M. Hamm, and O. Hess, "Negative-permeability electromagnetically induced transparent and magnetically active metamaterials," *Phys. Rev. B* **81**(19), 195128 (2010).
29. R. Singh, C. Rockstuhl, and W. Zhang, "Strong influence of packing density in terahertz metamaterials," *Appl. Phys. Lett.* **97**(24), 241108 (2010).

1. Introduction

Electromagnetic induced transparency (EIT) is an appealing physical phenomenon where the otherwise opaque medium becomes transparent for a probe laser if modified by a coupling laser beam [1]. In a three-state lambda scheme atomic system, EIT can be explained from destructive quantum interference between the two different excitation transition pathways: $|1\rangle\text{-}|2\rangle$, $|1\rangle\text{-}|2\rangle\text{-}|3\rangle\text{-}|2\rangle$, which thus gives rise to a sharp transparency window with extraordinarily steep normal dispersion in the broad absorption band. The strong dispersion is key to achieving a dramatic group-velocity reduction in propagating pulses and to realizing diverse effects. Since the discovery of EIT, a variety of intriguing applications have emerged including quantum nonlinear optics, slow light, ultrafast switching, optical data storage, signal processing, and optical delay lines [2,3]. Recently, mimicking EIT in classical metamaterial systems has attracted tremendous attention and various resonant schemes have been proposed and demonstrated to display the EIT-like spectral response [4]. In particular, with endowed strong optical response from subwavelength metallic structures, plasmon-induced transparency (PIT) is of great interest and becomes a promising addition to mimicking the EIT schemes [5]. A series of micro- and nano-structures have been taken into account to realize the PIT effect, such as cut wires [5], split-ring-resonators (SRRs) [6–8], coupled waveguide micro-resonators and other multi-layer structures [9–11]. These works have theoretically and experimentally demonstrated that the PIT effect can be realized in metamaterials via destructive interference between the superradiant and subradiant plasmonic modes or by breaking the symmetry of metamaterial system at microwave, terahertz, and optical frequencies [4–23].

Generally, an important rule in design of the PIT structures is that the chosen unit cell can excite two resonance modes with exactly identical resonance frequency but significantly

different quality factors (Q -factor). The PIT spectral response is therefore a result of coupling between a low- Q resonator and a high- Q resonator in a manner of destructive interference. In such a scheme, the PIT spectral response hinges on the coupling between the two constituent “atoms” and is thus sensitive to the structural configuration. In this article, we present a new type of PIT design in the terahertz regime with a systematic study of how the PIT spectral response can be controlled by changing the spatial configurations of “metamaterial molecules”. We experimentally and numerically demonstrate that the relative distance between two nearby constituent elements in the metamaterial structure plays a critical role in modifying the PIT spectral response in such a way that the transparency peak begins to disappear when the resonators are brought closer than a certain critical distance. This is in sharp contrast to the previously observed PIT effects in which the close distance between the superradiant and subradiant resonators led to enhanced transparency [5,6].

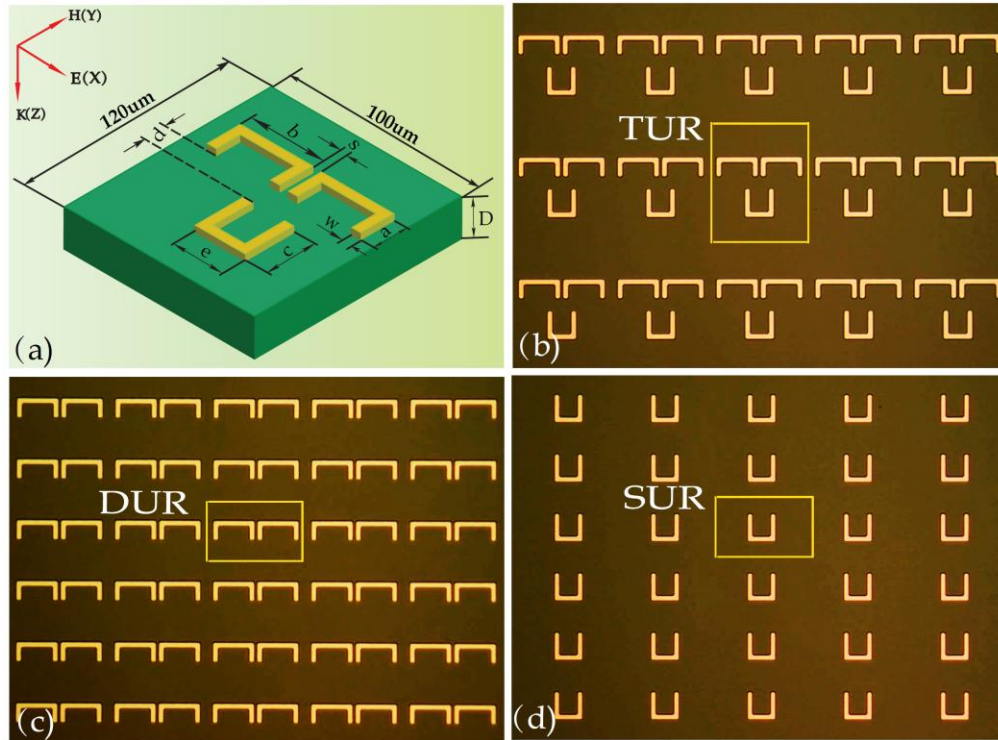


Fig. 1. (a) Geometric parameters of the proposed design: $a = 19 \mu\text{m}$, $b = 42 \mu\text{m}$, $c = 28 \mu\text{m}$, $e = 29 \mu\text{m}$, $s = 3 \mu\text{m}$, $w = 5 \mu\text{m}$, and $d = 12 \mu\text{m}$. The thickness of the aluminum microstructure is 200 nm . The period is $100 \mu\text{m}$ in the x direction and $120 \mu\text{m}$ in the y direction. The external electric field is along the x direction. (b)-(d) are optical images of the TURs, the sole-SURs and the sole-DURs samples characterized in the experiment, respectively.

2. Measured results and numerical analysis

The essence of our proposed PIT structure is a triple-U resonator (TUR) scheme consisting of a single-U resonator (SUR) and a double-U resonator (DUR) periodically printed on an isotropic dielectric substrate, as shown in Fig. 1. Within TURs, if the resonance frequencies ω for DURs and SURs are very close to frequency ω_0 , namely $\delta = \omega - \omega_0 \ll \omega_0$, the coupling between DURs and SURs may be established according to the coupling-mode theory as [13,16,22]:

$$\begin{pmatrix} \tilde{a} \\ \tilde{b} \end{pmatrix} = W(\omega)^{-1} \begin{pmatrix} p \tilde{E}_m \\ q \tilde{E}_m \end{pmatrix} = \begin{pmatrix} \delta - i\gamma_a & \kappa \\ \kappa & \delta - i\gamma_b \end{pmatrix}^{-1} \begin{pmatrix} p \tilde{E}_m \\ q \tilde{E}_m \end{pmatrix}, \quad (1)$$

where \tilde{a} and \tilde{b} represent the electric field amplitudes of DURs and SURs, respectively. γ_a (γ_b) is the damping factor of the DURs (SURs). p (q) is the parametric value indicating the coupling strength between the incident light \tilde{E}_m and DURs (SURs). The resonances of DURs and SURs are considered to be coupled to each other by a strength factor κ . To optimize the structure design, we make δ sufficiently small, p and q with appropriate values, and the resonances of DURs and SURs with strongly contrasting Q factors [23]. The coupling between the superradiant mode of DURs and subradiant mode of SURs induces the PIT effect. In our design here, 200-nm-thick Al TURs are fabricated by conventional photolithography on a silicon substrate (0.64-mm-thick, n-type) [24,25]. Figure 1(a) shows the diagram of a TUR unit cell, where the U-shape resonators are with geometric parameters $a = 19 \mu\text{m}$, $b = 42 \mu\text{m}$, $c = 28 \mu\text{m}$, $e = 29 \mu\text{m}$, $s = 3 \mu\text{m}$, $w = 5 \mu\text{m}$, and $d = 12 \mu\text{m}$. The TURs are printed, as shown in Fig. 1(b), on lattice periods of $100 \mu\text{m}$ along x axis and $120 \mu\text{m}$ along y axis. Within the proposed TUR structure, the SUR is designed to have long vertical arms and a short horizontal base, which can be regarded as a subradiant mode with a narrow linewidth at resonance. In contrast, the DUR possesses short vertical arms and long horizontal bases, which can be also considered analogous to a superradiant mode with a broad linewidth. For comparison, Figs. 1(c) and 1(d) show a sole-DUR and a sole-SUR sample with DURs/SURs printed on lattice periods of $100 \mu\text{m}$ along x axis and $60 \mu\text{m}$ along y axis. To measure the response of the structure, terahertz-time domain spectroscopy (THz-TDS) is used. The 8-f confocal THz-TDS system has a usable bandwidth of 0.1- 4.5 with a 3.5-mm-diameter beam waist which enables a frequency independent condition for small sample characterization [24,25].

The TURs are oriented parallel to the xy plane with the gaps of every U aligned to the y axis. The TURs would resonate if the incident electric field is oriented along the x axis (i.e. perpendicular to the gaps in each U). The amplitude transmission is extracted from the ratio of the Fourier transformed amplitude spectra of the sample to the reference, defined as $|\tilde{t}(\omega)| = |\tilde{E}_s(\omega)/\tilde{E}_r(\omega)|$, where $\tilde{E}_s(\omega)$ and $\tilde{E}_r(\omega)$ are Fourier transformed time traces of the transmitted electric field of the sample and reference (blank Si), respectively. Figures 2(a) and 2(c) illustrate the measured amplitude transmissions of the sole-SUR, the sole-DUR and the TUR samples, respectively. As shown in Fig. 2(a), both the sole-SUR and the sole-DUR samples exhibit strong resonance at the same frequency, but with significantly different Q factors, which obeys the aforementioned PIT design rule. Even though the SUR or DUR alone acts as a bright mode as their resonances are directly excited by incident field in a ‘‘TUR molecule’’, however, the SUR plays a role of a subradiant mode in the presence of a more strongly superradiant mode of the DUR. As a result, when these two different resonators are put together facing oppositely at a distance of $d = 12 \mu\text{m}$ to form a ‘‘TUR molecule’’, a typical PIT spectral response can be observed as shown in Fig. 2(c), where a sharp transmission peak appears at 0.75 THz between two resonance dips.

The measured characteristic spectral responses of the chosen structures are further supported by a full wave numerical simulation using CST Microwave Studio, as shown in Figs. 2(b) and 2(d). The unit cell shown in Fig. 1 was used in the simulations with periodic boundary condition. The substrate silicon was modeled as a lossless dielectric $\epsilon = 11.78$ and Al was simulated with a default conductivity of $\sigma = 3.72 \times 10^7 \text{ S}\cdot\text{m}^{-1}$. The simulations reveal a good agreement with the experimental results.

Figures 2(e), 2(f) and 2(g) depict the surface current of the sole SUR, the sole DUR and the TUR samples, respectively. It is found that both the sole-SUR and the sole-DUR samples have strong current oscillations directly excited by the incident terahertz field. However, in the TURs, the surface currents of the constituent DURs appear to be suppressed due to the nearest neighbor interaction with the constituent SURs, as shown in Fig. 2(g). In another words, in the TURs, resonant excitation of the DUR mode is suppressed due to the coupling between the DUR and the SUR. The interaction between these two resonators leads to the formation of two new modes (two dips in the spectra) and thus opens up a transparency window. More specifically, as the incident wave is polarized in the x direction, it tends to drive the bases of both the SURs and the DURs to produce surface current oscillations in the same direction, but the excited fields of the SURs intend to induce a surface current of opposite-direction in the DURs. Therefore, anti-parallel oscillating charges from external field and the coupled SURs (subradiant mode) have a destructive superposition in the DURs (superradiant mode), thus leading to the suppressed currents in the DURs [10,26].

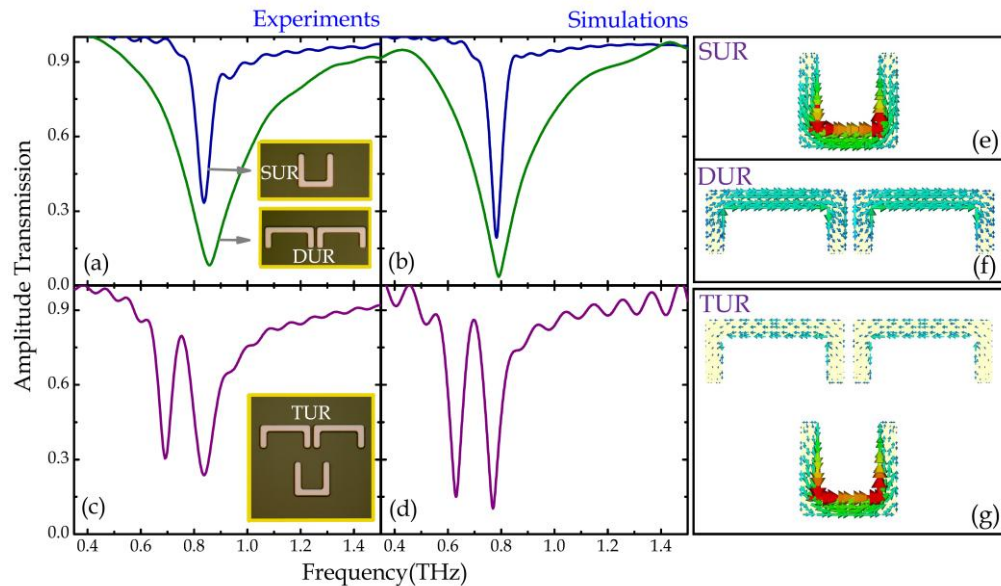


Fig. 2. (a) Measured and (b) simulated amplitude transmission spectra of the sole-SUR and the sole-DUR samples. (c) Measured and (d) simulated amplitude transmission spectra of the TUR sample. (e), (f) and (g) are calculated surface currents.

To gain more insight on the influence of destructive coupling between the SURs and the DURs on the PIT spectral response of the proposed TUR structure, we have further characterized different TUR samples with various relative vertical and horizontal distances between the SURs and the DURs.

In the first case, when we reduce the vertical distance d between the SURs and the DURs from 12 to $-10 \mu\text{m}$, it is interesting to see that the PIT window disappears gradually, as shown in Fig. 3(a). Figure 3(b) represents the corresponding simulated spectra and the overall qualitative agreement between the experimental and simulated results is good.

To highlight the underlying physics of the measured spectra with varying separation d , current densities and field distributions at the resonance transparency peak are given in Fig. 4. It is evident that with reducing d , the current densities and electric field distributions in the DURs change drastically. When the SUR and DUR are brought closer with reducing d , the inner-arms of the DUR tend to couple more strongly with the arms of the SUR, causing the suppression of currents in the SUR and enhancement of currents in the DUR. As shown in

Fig. 4, we observe that there is a gradual transfer of electromagnetic energy from the SUR to the DUR. For the sample with $d = 12 \mu\text{m}$, most of the energy is concentrated in the SUR. As d is decreased to $0 \mu\text{m}$, the electromagnetic energy is distributed almost uniformly on the DUR and the SUR. Further reducing d to $-10 \mu\text{m}$, more energy seems to be gradually transferred from the SUR and localized only on DUR. Consequently, on one hand, the DUR becomes highly radiative whereas on the other hand the resonance of SUR which acts as a subradiant resonator is completely quenched, such that the PIT response disappears.

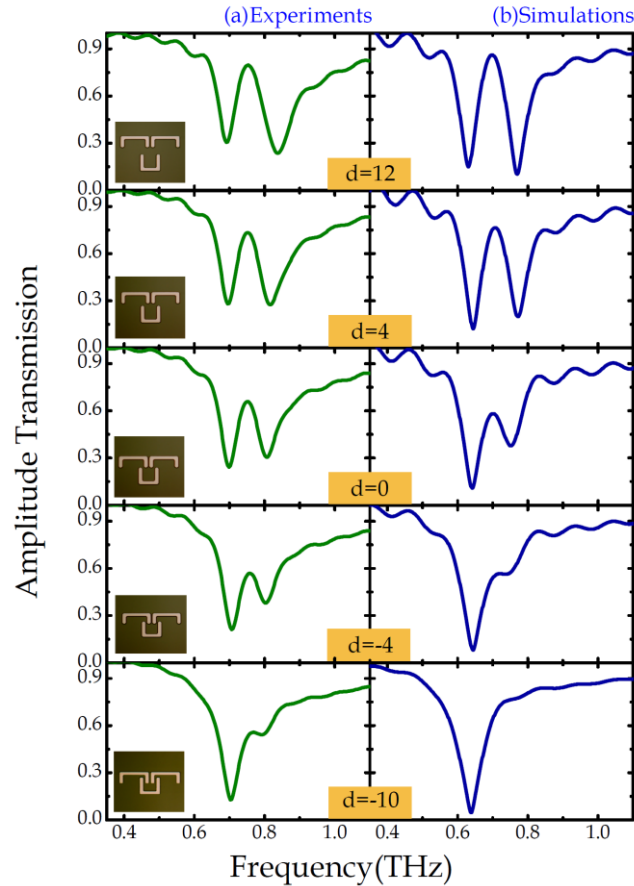


Fig. 3. (a) Measured and (b) simulated transmission spectra for different vertical separation distances d between the SUR and the DUR in the TUR unit cell.

In addition, another scheme is implemented by horizontally moving the position of SUR atom in the TUR molecule. The measured spectra are shown in Fig. 5(a) for various relative horizontal displacement distances h . The corresponding simulated spectra are well reproduced in Fig. 5(b). As illustrated in Figs. 5(a) and 5(b), when h varies from 0 to $30 \mu\text{m}$, we found that the transmission peak is nearly undisturbed and no remarkable differences are observed. In this case, we noticed that the surface current of each U-shape resonator in the DURs is quite different, as shown in the inset of Fig. 5(b): the surface current of the right-U resonator is considerably stronger than that of the left one. The distinct surface currents of these two U resonators in the DUR further verify the opposite direction excitation provided by the scattered electric field of the SUR (subradiant mode), which renders the right-U resonator in the DUR to be strongly excited while the left one being in a more suppressed state due to the superposition of excitation from the SUR and the external field.

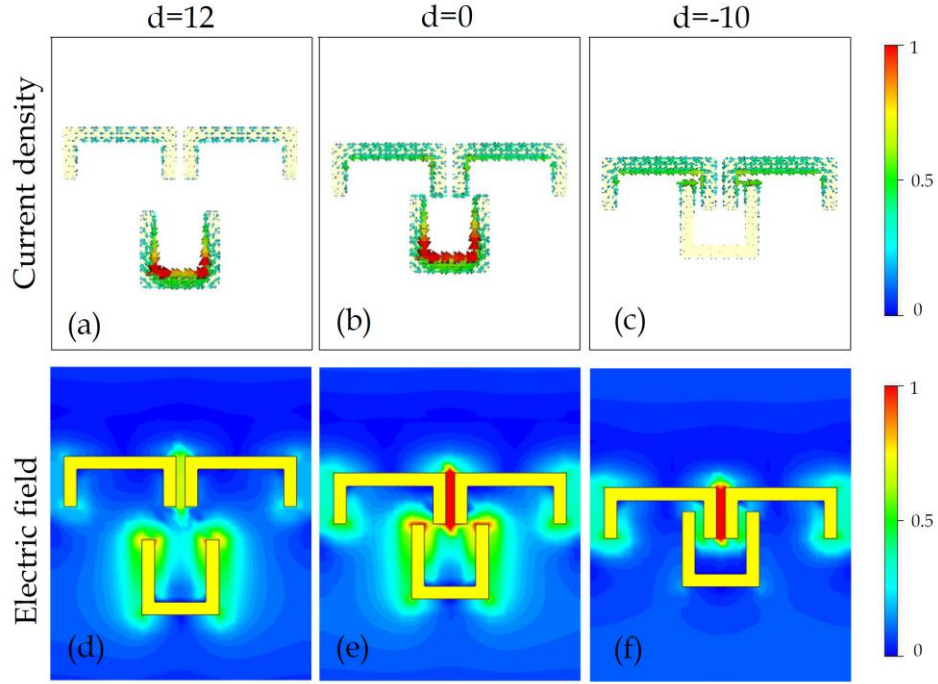


Fig. 4. Current densities and electric field distributions of the proposed structures with various d of 12, 0 and $-10 \mu\text{m}$, respectively.

In order to obtain more threads of the aforementioned modulation process in the PIT spectra, we develop the coupling-mode theory as a function of the coupled circuit parameters, where the coupled resonators are modeled by the equivalent RLC circuits [7,13]. Figure 5(c) shows the equivalent RLC circuits: two RLC resonators P_1 and P_2 are coupled by a common effective capacitor C_C [27,28]. The inductive coupling between the RLC resonators has not been considered here as the magnetic coupling between the closely spaced SRRs are very weak [29]. Here P_1 (P_2) represents the equivalent circuit resonator of DUR (SUR) and C_C represents the equivalent coupling function between the two modes. The voltage sources in the upper and lower subcircuits correspond to the external incident field. The resonance currents I_1 and I_2 circulating in P_1 and P_2 circuit loops can be calculated based on standard loop current analysis:

$$\begin{pmatrix} \tilde{I}_1 \\ \tilde{I}_2 \end{pmatrix} = Z(\omega)^{-1} \begin{pmatrix} p\tilde{U}_{in} \\ q\tilde{U}_{in} \end{pmatrix} = \begin{pmatrix} -j\omega L_1 + R_1 + \frac{1}{-j\omega C_1} & \frac{1}{-j\omega C_C} \\ \frac{1}{-j\omega C_C} & -j\omega L_2 + R_2 + \frac{1}{-j\omega C_2} \end{pmatrix}^{-1} \begin{pmatrix} p\tilde{U}_{in} \\ q\tilde{U}_{in} \end{pmatrix}, \quad (2)$$

By comparing Eqs. (1) with (2), we note that the coupling matrix W is proportional to the impedance matrix Z and the coupling strength factor k is proportional to $\left| \frac{1}{-j\omega C_C} \right|$. In the first

case involving decrease of d , the common effective capacitance C_C is increased due to decreased effective distance between equivalent capacitance plates of the DUR and the SUR. Consequently, we have a reduced coupling factor k with decreasing d . Since the coupling between the DUR and SUR is reduced in spite of the close physical proximity of the resonators, the DUR is free from the suppressed state, making it highly radiative while the

currents in SUR completely disappear, quenching its fundamental resonance, thus leading to the disappearance of the PIT peak. When we vary the horizontal displacement parameter h , neither the effective vertical distance nor the dimension of capacitance plates is significantly altered, so the pronounced PIT spectra do not display any significant changes.

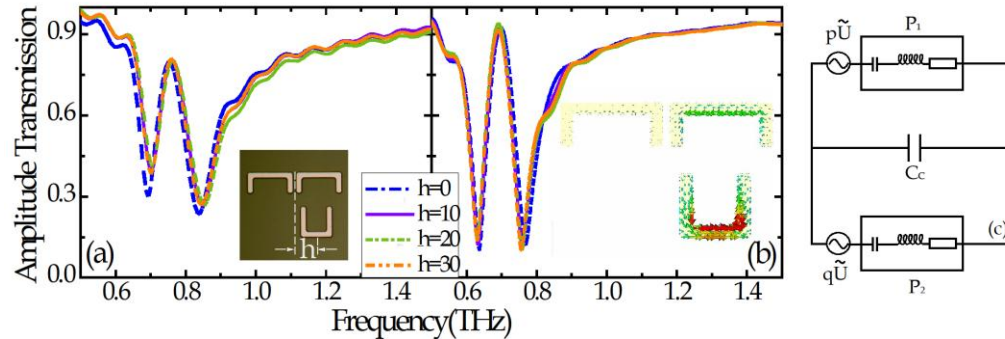


Fig. 5. (a) Measured and (b) simulated transmission spectra for different horizontal movement h . The inset of (b) is the surface current oscillation of the asymmetric TUR induced by horizontal displacement. (c) The equivalent RLC circuits.

3. Conclusion

In conclusion, we experimentally and numerically demonstrate that the TUR metamaterial consisting of the SUR and DUR constituent resonators exhibits a tunable PIT spectral response at terahertz frequencies. The effects of vertical and horizontal separations between the resonators on the PIT behaviors are systematically studied, indicating that the PIT spectral response can be engineered by varying the relative vertical distance between the subradiant and superradiant resonators. A counterintuitive phenomenon is observed, i.e. when the subradiant and superradiant resonators were brought closer to each other in the vertical direction, the transparency peak begins to gradually disappear beyond a critical distance of separation. This effect is mainly due to complete suppression of resonance in the subradiant resonators and enhanced radiative nature of the superradiant resonators as they are coupled at a close vertical distance. In the case of horizontal displacement, however, the transparency peak remains uninterrupted as the field distributions are not affected. The vertical coupling effect can tune the PIT behavior and thus could lead to promising applications in slow light devices in the terahertz regime.

Acknowledgments

This work was supported by the National Natural Science Foundation of China (NSFC) (Grant Nos. 61028011, 61007034, and 60977064), the U.S. National Science Foundation, the Tianjin Sci-Tech Program (Grant Nos. 09ZCKFGX01500 and 10JCYBJC01400), and the MOE 111 Program of China (Grant No. B07014).